

## Oxidation of terpenic alcohols with hydrogen peroxide promoted by Nb<sub>2</sub>O<sub>5</sub> obtained by microwave-assisted hydrothermal method



Daniel Carreira Batalha<sup>a</sup>, Natália Hadler Marins<sup>b</sup>, Ricardo Marques e Silva<sup>b</sup>, Neftalí Lenin Villarreal Carreño<sup>b</sup>, Humberto Vieira Fajardo<sup>c</sup>, Márcio José da Silva<sup>a,\*</sup>

<sup>a</sup> Chemistry Department, Federal University of Viçosa, Viçosa, Minas Gerais, 36570-900, Brazil

<sup>b</sup> Graduate Program in Materials Science and Engineering, Technology Development Center, Federal University of Pelotas, Pelotas, Rio Grande Do Sul, 96010-610, Brazil

<sup>c</sup> Chemistry Department, Institute of Exact and Biological Sciences, Federal University of Ouro Preto, Ouro Preto, Minas Gerais, 35400-000, Brazil

### ARTICLE INFO

#### Keywords:

Niobium oxide  
Heterogeneous catalysis  
Hydrogen peroxide  
Nerol

### ABSTRACT

The present work describes the synthesis of niobium oxides by microwave-assisted hydrothermal method and their evaluation as a solid catalyst in oxidation reactions of terpenic alcohols with hydrogen peroxide. Effects of main parameters of synthesis were assessed and all the prepared catalysts were characterized by physical adsorption/desorption analyses of nitrogen, infrared and Raman spectroscopies, scanning electron microscopy and powder X-rays diffraction analyses. The strength and number of acidic sites of the catalysts were determined by potentiometric titration. Morphological and structural characterization corroborate with the activity and selectivity achieved by the niobium oxides. The reusability of the catalyst was evaluated. The impacts of main reaction variables such as temperature, catalyst, and oxidant load were assessed. Niobium oxide demonstrated to be an effective catalyst, selectively converting the nerol (model molecule) to epoxide and aldehyde. Oxidation of various terpenic alcohols was investigated. Only geraniol and nerol were selectively epoxidized, suggesting a hydroxyl group assisted reaction. Although being also allylic alcohol, linalool was unreactive toward epoxidation due to the presence of a methyl group at the same carbon atom than the hydroxy group. The use of an environmentally cheap friendly oxidant (H<sub>2</sub>O<sub>2</sub>) and efficient solid catalyst (Nb<sub>2</sub>O<sub>5</sub>) are positive aspects of this process.

### Introduction

The conversion of abundant and renewable raw materials to high value-added chemicals assumed great importance due to economic and environmental reasons [1–3]. Fine chemicals, pharmaceutical, and fragrance industries are each time more dependent on sustainable processes that use friendly reactants, recyclable catalysts, and inexpensive feedstocks [4,5].

Among the natural origin feedstock, monoterpenes deserve to be highlighted due to wide application as an ingredient of perfumes, flavors, and food, all motivated by their attractive organoleptic properties [6–8]. Terpenic alcohol derivatives as epoxides are building block in synthesis of chiral compounds, while carbonyl products as aldehydes and ketones are valuable ingredients of perfume, whose obtention per pass through oxidative processes where clean oxidant and solid catalysts are highly desirable [9–12]. However, the presence of two oxidizable sites in terpenic alcohols (i.e., the double bond and a hydroxyl

group) may hamper the control of the reaction selectivity [13].

Green oxidants as hydrogen peroxide are very appealing; similarly to the molecular oxygen, it generates water as an only by-product. However, unlikely molecular oxygen, it has the advantage to be liquid, and not flammable at room conditions. Moreover, it is soluble in water and polar solvents, safe handling, and it is a cost-effective and atom-efficient oxidant [14,15]. When used in the presence of solid catalysts, hydrogen peroxide can interact with the catalyst surface and induce homo- or heterolytic cleavage of O–O bond in H<sub>2</sub>O<sub>2</sub>, which may generate different oxidative species [16,17].

The direct oxidation of olefin or alcohol by hydrogen peroxide is always kinetically unfavored and impeded by the high energy barrier of the oxygen transfer reaction from oxidant to the substrate [18,19]. Thus, several catalysts that facilitate the oxidation providing a low-energy pathway, have been proposed. In special, various metal oxides or salt-based catalysts have demonstrated to be active in either oxidation or epoxidation reactions [20–22].

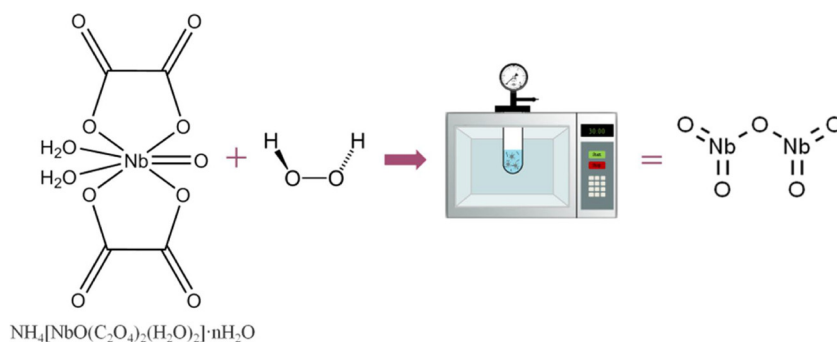
\* Corresponding author at: Chemistry Department, Federal University of Viçosa, Campus Universitário, Avenue P.H. Rolfs, s/n, Viçosa, Minas Gerais State, CEP: 36570-000, Brazil.

E-mail address: [silvamj2003@ufv.br](mailto:silvamj2003@ufv.br) (M.J. da Silva).

<https://doi.org/10.1016/j.mcat.2020.110941>

Received 11 January 2020; Received in revised form 17 March 2020; Accepted 30 March 2020

2468-8231/© 2020 Elsevier B.V. All rights reserved.



**Scheme 1.**  $\text{Nb}_2\text{O}_5$  synthesis by microwave-assisted hydrothermal method.

The use of a heterogeneous catalyst leads to a cleaner process, since it reduces the waste generation, allows the recovery and the reuse of the catalyst, and diminish the cost of the processes. Different strategies have been proposed to obtain efficient heterogeneous catalysts in epoxidation or oxidation reactions of functionalized olefins with hydrogen peroxide. For a long time,  $\text{Ti}/\text{SiO}_2$  catalysts have been preferred in the epoxidation of terpenic alcohols [23]. Mixed oxides, solid-supported metals, framework-substituted molecular sieves, and modified mesoporous silica are also examples of catalysts active on these reactions [24–26].

Nevertheless, in reactions that use heterogenized homogeneous catalysts, the leaching provoked by the high polarity of the reactants (i.e., aqueous hydrogen peroxide) is always an obstacle that may compromise the reuse of the catalyst. Therefore, the development of a stable, recyclable, and truly heterogeneous catalyst, which achieves epoxidation rates and selectivity likewise the homogeneous counterparts is still a challenge to be overcome. Recently, to circumvent the leaching of the active phase in solid catalysts, we have synthesized insoluble Keggin heteropolyacid salts, which were successfully tested as catalysts in terpenic alcohol oxidation reactions with hydrogen peroxide [27].

The use of solid metal oxide as the catalyst excludes the possibility of leaching. Niobium oxide has desirable properties to be used as a heterogeneous catalyst. It has a high surface area and good thermal stability. Moreover,  $\text{Nb}_2\text{O}_5$  has Brønsted and Lewis acidic sites in their structure, being potentially a bifunctional catalyst [28]. Niobium-containing catalysts can be prepared in several routes such as sol-gel, grafting, hydrothermal, coprecipitation, or polymeric precursor methods [29–32]. The treatment of niobium catalysts with hydrogen peroxide is a strategy that improves their activity in oxidation reactions [33].

Due to these features, niobium oxide has been an efficient catalyst in different oxidation reactions. Nanoparticles of niobium oxide were synthesized through microwave-assisted method and used as catalysts in aniline oxidation reactions with hydrogen peroxide in liquid phase [34]. The same reaction was also efficiently performed when  $\text{Al}_2\text{O}_3/\text{AlNbO}_4$  were applied as the catalyst [35]. Cerium-chromium-niobium oxides were successfully evaluated in processes to deep oxidation of dichloroethane, demonstrating have potential industrial application [36]. Conversely, the high acidity of niobium oxides makes them efficient and reusable acid catalysts in xylose dehydration processes to furfural production [37].

In this work, niobium oxides were prepared by microwave-assisted hydrothermal method and evaluated in oxidation reactions of terpenic alcohols with hydrogen peroxide. The impacts of the temperature of synthesis on the physical and structural properties of niobium oxides were assessed. The solid catalysts were characterized by FT-IR and Raman spectroscopy analyses, physical adsorption/desorption of nitrogen, thermogravimetry and powder XRD analyses. Acidity properties were determined by *n*-butylamine potentiometric titration. The nerol oxidation was studied in detail. The effects of main reaction parameters

such as temperature, oxidant, and catalyst loads were also investigated. Special attention was paid to describe the reaction mechanism. The reaction scope was also extended to other terpenic alcohols.

## Experimental

### Catalyst preparation

$\text{Nb}_2\text{O}_5$  was synthesized by microwave-assisted hydrothermal method as previously described [38,39]. Ammonium niobium oxalate was dispersed in distilled water under stirring for 30 min. Following, hydrogen peroxide was dropped in the solution and stirred for 30 min. The final solution was poured into a Teflon autoclave and placed in a microwave oven (Electrolux, MEF41, Brazil). The catalysts were synthesized at 433 K for different times (2, 4, and 8 h) under the constant pressure of 85 psi. After cooling, the precipitate was washed with absolute ethanol (LabSynth, Brazil), and dried in an oven (DeLeo, A5SE, Brazil) at 323 K for 24 h under air atmosphere. The Scheme 1 below shows briefly the niobium oxides synthesis used as catalysts.

### Catalyst characterization

Textural properties of niobium oxides were obtained at 77 K in a NOVA 1200 Quantachrome equipment. The Brunauer-Emmett-Teller equation was applied to the isotherms of adsorption/desorption of  $\text{N}_2$ , which provided the surface area of the solids. Diameter and pore volume distribution was calculated according to the DFT method. The morphologies of the catalysts were investigated by scanning electron microscopy (SEM) using a microscope SSX-550, SHIMADZU, Japan.

Infrared spectroscopy analyses were performed in KBr pellets using an ABB Bomen MB 3000 FTIR spectrometer (Quebec, Canada) equipped with ZnSe optics and a deuterated triglycine sulfate (DTGS) detector set at a  $4\text{ cm}^{-1}$  resolution and wavenumber range of  $400\text{--}4000\text{ cm}^{-1}$ .

XRD pattern of the  $\text{Nb}_2\text{O}_5$  powders was analyzed by X-ray diffraction (Shimadzu, XRD 6000, Japan), using a diffractometer with  $\text{CuK}\alpha$  radiation ( $\lambda = 1.5418\text{ \AA}$ ), and a scan range of  $20\text{--}70^\circ$ . Crystallite sizes were calculated using the Scherrer equation:

$$L = \frac{K \cdot \lambda}{\beta \cdot \cos\theta} \quad (1)$$

Where  $\lambda$  is the X-ray wavelength in nanometer (nm),  $\beta$  is the peak width of the diffraction at half maximum height resulting from small crystallite size in radians, and  $K$  is a constant related to crystallite shape, normally taken as 0.89.

Raman spectra were recorded in a Horiba/Jobin-Yvon Labram-HR spectrometer equipped with He-Ne laser (laser excitation lines of 632.8 nm and 18 mW of power) and an Olympus microscope. The analyses were carried out with an acquisition time of 5 s with 10 accumulations in the region of  $60\text{--}1200\text{ cm}^{-1}$  and a 100x microscope objective.

The amount and strength of the acidic sites of niobium oxides were determined by *n*-butylamine potentiometric titration using a BEL

potentiometer (model W3B) with a glass electrode. Typically, 50 mg of Nb<sub>2</sub>O<sub>5</sub> was suspended in CH<sub>3</sub>CN (ca. 30 mL) and magnetically stirred for 3 h. Posteriorly, the suspension was titrated with slow addition of portions of *n*-butylamine (ca. 0.025 mol L<sup>-1</sup>) until that the electrode potential remained stable after the addition of the titrant again.

#### Catalytic tests

Oxidation reactions were carried out in liquid phase using a glass reactor fitted (ca. 50 mL) with a reflux condenser and sampling septum, in a glycerin batch under magnetic stir and heating. Typically, H<sub>2</sub>O<sub>2(aq)</sub> (ca. 35 wt. %) and nerol (1.375 mmol) were dissolved in CH<sub>3</sub>CN (ca. 10 mL) and heated to 333 K. The addition of niobium started the reaction, which proceeded for 8 h.

Aliquots were collected at regular time intervals. Before the analysis, the aliquots were centrifuged, and the supernatant was analyzed on a GC-2010 Plus Shimadzu Gas Chromatograph with a flame ionization detector (FID), equipped with an auto-injector AOC-20i, and fitted with a capillary column Rtx®-Wax (30 m x 0.25 mmID x 0.25 μm). The chromatographic conditions were initial temperature (353 K / 3 min), heating rate (10 K / min until 493 K), which was kept constant 3 min. Injector and detector temperatures were 523 K and 523 K, respectively. Nitrogen was the carrier gas (1.2 ml / min).

## Results and discussion

#### Catalysts characterization

Table 1 shows the surface area, volume, and pore diameter values quantified by the BET and DFT methods of Nb<sub>2</sub>O<sub>5</sub> catalysts.

An increase in the time of synthesis resulted in an improvement of surface area and a higher volume of pores. Conversely, pores diameters were lower when longer times were used. This effect was also verified by us in a previous work [39]. We can consider that each rod that compose this material is composed of several rods with smaller diameters. The synthesis time influences the rods growth; if a greater time of synthesis is used, larger will be the size of the stem. As a result, may occur an increase in surface area and pore volume [39].

The catalyst Nb<sub>2</sub>O<sub>5</sub> - 2 h presented the lowest values of surface area and pore volume but showed a larger value in its diameter, above 30 Å, characteristic of a mesoporous material. In contrast, the two other oxides showed an increasing on the surface area and pore volume when the synthesis time was increased. Since pore diameter was reduced to values lower than 20 Å, we can conclude that micropores were formed in the materials [38,39].

Fig. 1 shows the physical adsorption/desorption isotherms of N<sub>2</sub> and pore diameter distributions. According to IUPAC recommendations, the isotherms of the synthesized salts can be classified as type V, characteristic of microporous and mesoporous materials.

The hysteresis observed in the isotherm curves can be classified as H3 type, which is typical of plate-shaped particle aggregates giving rise to slit pores [40]. According to the pore diameter distribution curve profiles, the niobium oxides synthesized presented diameters in the range of micro and mesoporous.

FT-IR spectra presented bands at approximately 1100 cm<sup>-1</sup> that were assigned to the asymmetric stretching of Nb–O–Nb bonds (Fig. 2)

**Table 1**  
Characterization of the catalysts through the physical adsorption of nitrogen<sup>a</sup>.

| Catalyst                             | S <sub>BET</sub> (m <sup>2</sup> /g) | V <sub>DFT</sub> (cm <sup>3</sup> /g) | D (Å) |
|--------------------------------------|--------------------------------------|---------------------------------------|-------|
| Nb <sub>2</sub> O <sub>5</sub> - 2 h | 17.4                                 | 0.035                                 | 31.7  |
| Nb <sub>2</sub> O <sub>5</sub> - 4 h | 107.4                                | 0.095                                 | 16.9  |
| Nb <sub>2</sub> O <sub>5</sub> - 8 h | 215.9                                | 0.340                                 | 16.9  |

<sup>a</sup> S<sub>BET</sub> = surface area; V<sub>DFT</sub> = cumulative pore volume; D = pore diameter.

[41,42]. The broad band at 3600–3200 cm<sup>-1</sup> regions refers to the vibration modes of hydrogen-bonded hydroxyl groups. The presence of bands at 1700 cm<sup>-1</sup> reinforces the Nb-linked OH- groups.

It is noteworthy that the intensities of the bands in this last region varied according to the synthesis time, suggesting that shorter synthesis times favored a higher presence of the hydroxyl groups. The ability of these groups to bind to H<sub>2</sub>O<sub>2</sub> molecules generating different reactive oxygen species may improve the activity of these niobium oxides in oxidation reactions [41,43].

Fig. 3 represents the X-rays diffractograms of the three synthesized catalysts. The literature describes the existence of four different phases for Nb<sub>2</sub>O<sub>5</sub>: Nb<sub>2</sub>O<sub>5</sub>.*n*H<sub>2</sub>O (amorphous), TT-Nb<sub>2</sub>O<sub>5</sub> (hexagonal), T-Nb<sub>2</sub>O<sub>5</sub> (orthorhombic) and H-Nb<sub>2</sub>O<sub>5</sub> (monoclinic) [44]. The diffractograms revealed by XRD analyses indicate the peaks are related to the hexagonal phase (JCPDS No. 28-0317) [39]. The broad peak noticed at 26° is assigned to the amorphous phase due to the use of hydrated starting materials and water. The presence of weak peaks is due to the low temperature used in the synthesis, which influenced their crystallinity [45,46]. The Nb<sub>2</sub>O<sub>5</sub> samples of 2 h, 4 h, and 8 h exhibited crystallite sizes of 12.7 nm, 14.8 nm, and 15.1 nm, respectively.

Fig. 4 presents the Raman spectra of the three Nb<sub>2</sub>O<sub>5</sub> samples. It was found that they had distinct profiles, indicating the presence of more than one phase in each material. Bands in the region of 200–300 cm<sup>-1</sup> were assigned to the stretching of Nb–O–Nb bonds [46].

The absorption bands in the 570–770 cm<sup>-1</sup> region refer to the symmetrical stretching modes of the Nb–O bonds (NbO<sub>6</sub>, NbO<sub>7</sub>, and NbO<sub>8</sub>) [46,47]. For the two samples synthesized in shorter time, 2 and 4 h, the single band in this region may indicate the greater presence of the amorphous phase. For the catalyst synthesized for 8 h, this band has a small shoulder closer to 700 cm<sup>-1</sup>, which may indicate the greater formation of the orthorhombic phase due to longer synthesis time [48]. This indicates that the time of synthesis affected the proportion between these two phases.

The broad band more pronounced in the spectra of catalysts synthesized at 2 and 4 h, present in the 900–1000 cm<sup>-1</sup> region, were assigned to the symmetrical and asymmetrical stretching of terminal bonds Nb = O, which is associated with Lewis acid sites [47]. This stretching band is related to the crystallinity degree of the sample; the more intense is the band, the lower is the crystallinity and more acid is the material [47–49]. This same phenomenon is little noticed for the sample synthesized for 8 h, confirming the higher crystallinity and may indicate a lower number of Lewis acid sites for this material.

The lower crystallinity degree of the Nb<sub>2</sub>O<sub>5</sub> - 2 h catalyst can be verified by the XRD graph. Comparing the results shown by XRD and IR, it should be noted the shorter is the catalyst synthesis times, the lower is the crystallinity and more intense is the OH<sup>-</sup> grouping bands in IR spectra. According to Ziolk et al, the activity for niobium oxides varies according to its crystallinity, being a parameter proportional to the number of hydroxyl groups present on the catalyst surface [17,43].

Fig. 5 shows the potentiometric titration curves of three synthesized niobium oxides. The initial electrode potential (E<sub>i</sub>) indicates the maximum acidity strength and the total number of acidic sites being provided by the inflection value of titration curve (ca. mEq *n*-butylamine / g catalyst), which was obtained from the minimum of the first derivative of each titration curve. The strength of the sites can be classified according to the scale: E<sub>i</sub> > 100 mV (very strong), 0 < E<sub>i</sub> < 100 mV (strong), -100 < E<sub>i</sub> < 0 mV (weak) e E<sub>i</sub> < -100 mV (very weak) [50].

All the niobium catalysts presented very strong acidic sites as demonstrated by the high E<sub>i</sub> values showed in Fig. 5, which was higher than 100 mV. Moreover, as higher the synthesis time, lower was the acidity strength. The number of total acidic sites (ca. mEq of *n*-butylamine/ g of catalyst) followed the order 0.95, 0.45, and 0.40 for Nb<sub>2</sub>O<sub>5</sub> - 2 h, Nb<sub>2</sub>O<sub>5</sub> - 4 h and Nb<sub>2</sub>O<sub>5</sub> - 8 h oxides, respectively. Therefore, the solid Nb<sub>2</sub>O<sub>5</sub> - 2 h showed both the strongest acid sites and the greatest number of total acidic sites.

It is important to highlight that the results of potentiometric

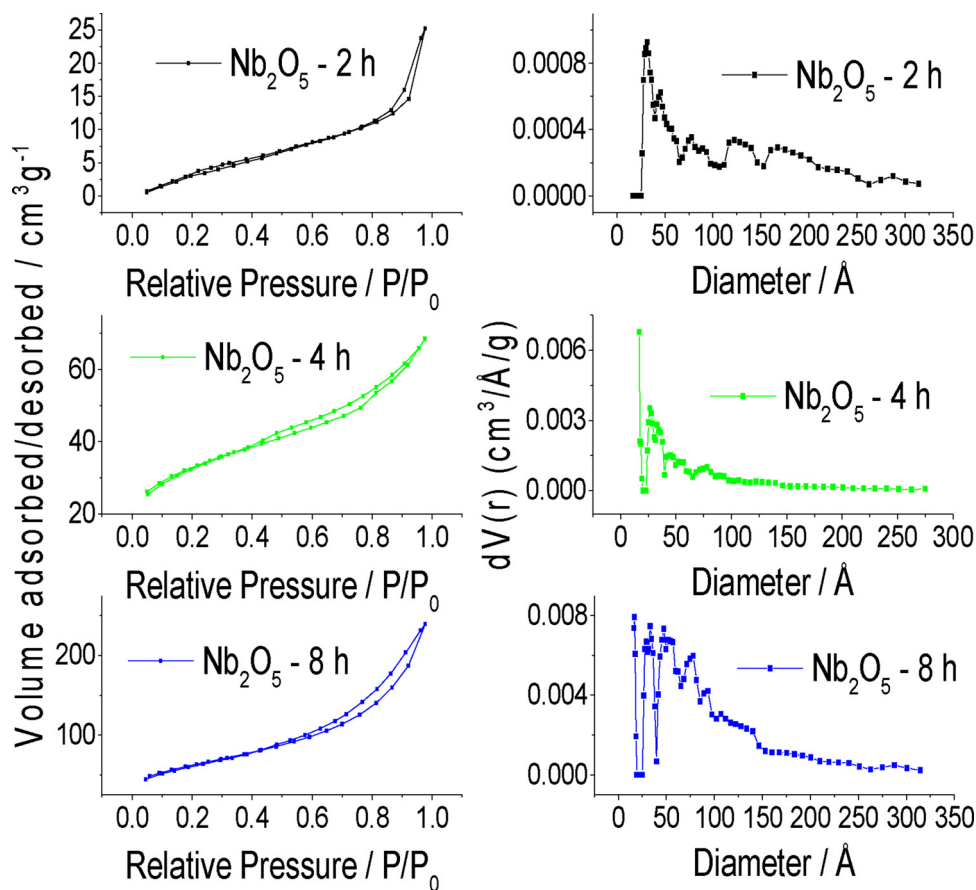


Fig. 1. Isotherms of physical adsorption/desorption of  $N_2$  and pore diameter distribution for niobium oxides.

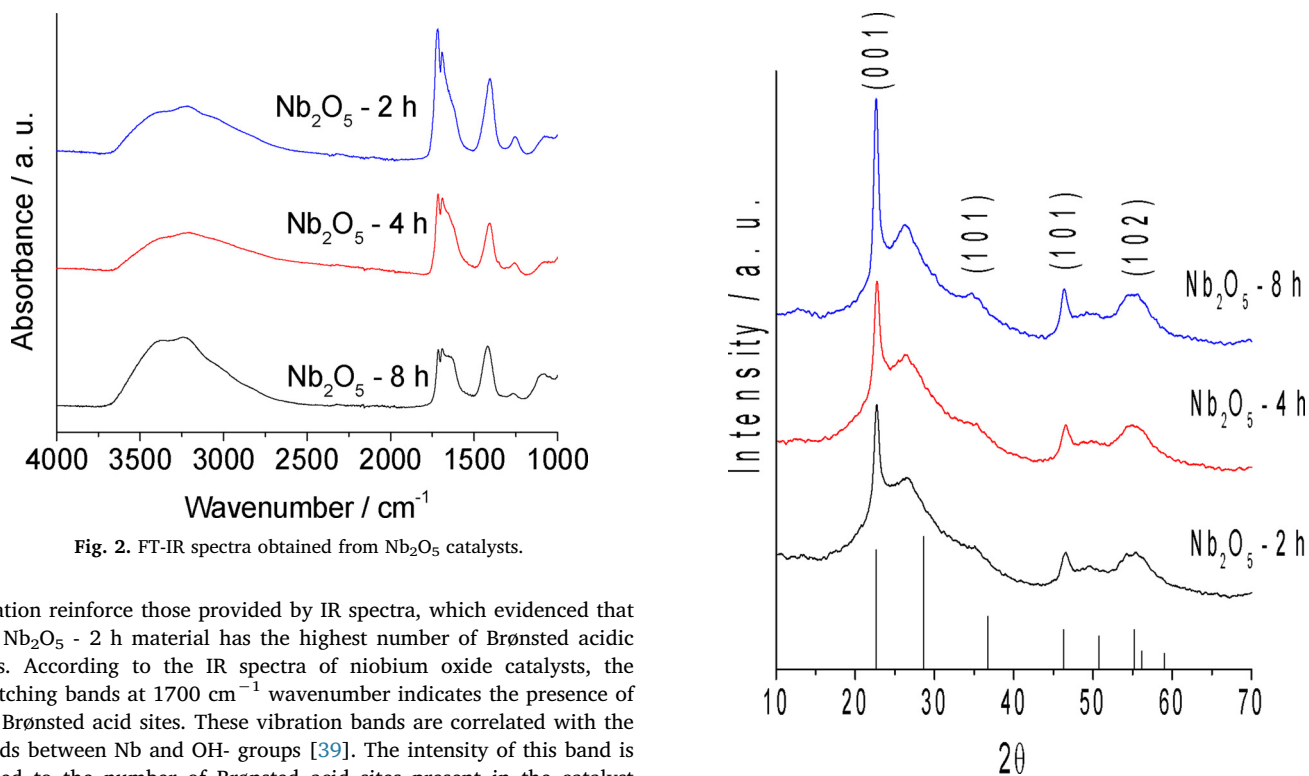


Fig. 2. FT-IR spectra obtained from  $Nb_2O_5$  catalysts.

titration reinforce those provided by IR spectra, which evidenced that the  $Nb_2O_5$  - 2 h material has the highest number of Brønsted acidic sites. According to the IR spectra of niobium oxide catalysts, the stretching bands at  $1700\text{ cm}^{-1}$  wavenumber indicates the presence of the Brønsted acid sites. These vibration bands are correlated with the bonds between Nb and OH- groups [39]. The intensity of this band is linked to the number of Brønsted acid sites present in the catalyst surface. As can be seen, the  $Nb_2O_5$  - 2 h catalyst presented the highest number of acid sites (ca. 095) and the more intense vibration band at  $1700\text{ cm}^{-1}$  wavenumber (see Fig. 2).

Fig. 3. Powder XRD patterns of  $Nb_2O_5$  synthesized at different times.

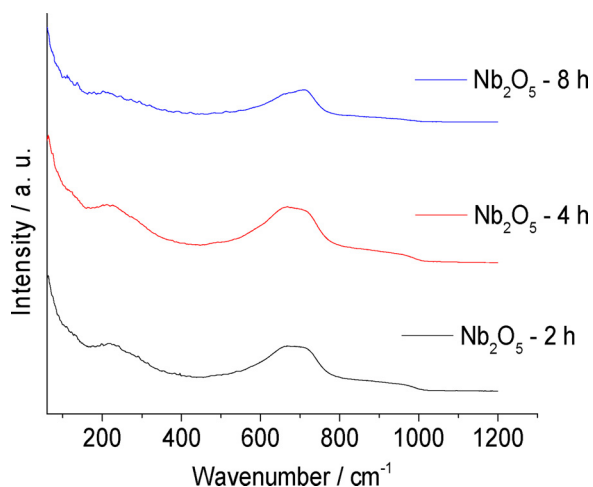


Fig. 4. Raman spectra of the three different synthesized niobium.

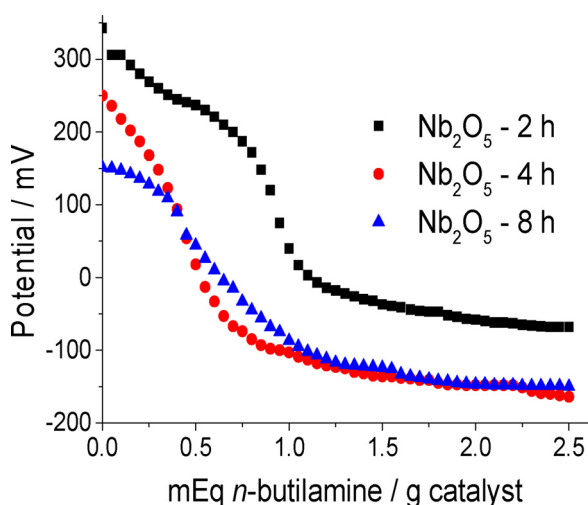


Fig. 5. Potentiometric titration curves with *n*-butylamine of the niobium oxides.

Fig. 6 shows SEM micrographs of synthesized niobium oxides. The Nb<sub>2</sub>O<sub>5</sub> particles were moderately aggregated and exhibited an approximately spherical shape, regardless of the synthesis times. Although this aspect it is not totally clear on the SEM images, previous works showed that this material presented a spherical shape [39].

The morphologies varied with an increase of hydrothermal treatment. At longer synthesis times, materials roughness increases. Although the SEM images are unable to provide information about the pores size, we have found that the formation of particles with larger surface area and high pore volume was obtained when a longer synthesis time was used [39,51]. The BET analyses and porosimetry

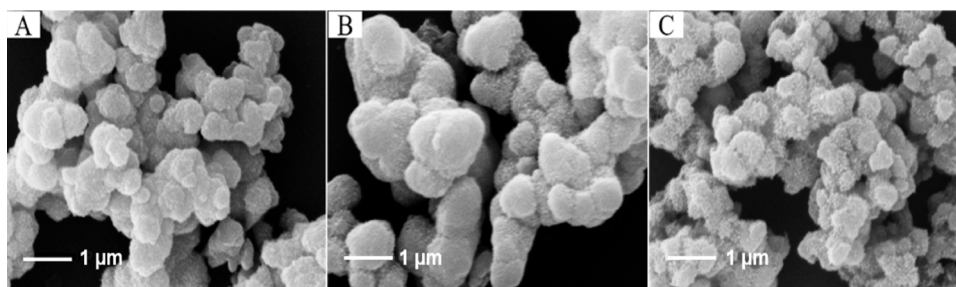


Fig. 6. SEM micrographs at x15000 magnification of Nb<sub>2</sub>O<sub>5</sub> - 2 h (A), Nb<sub>2</sub>O<sub>5</sub> - 4 h (B), and Nb<sub>2</sub>O<sub>5</sub> - 8 h (C) catalysts.

support this conclusion (Table 1).

#### Catalytic tests

##### An initial screening of niobium catalysts

The catalytic performance of synthesized niobium oxides was assessed in the nerol oxidation reaction with H<sub>2</sub>O<sub>2</sub>. Fig. 7 displays the kinetic curves and selectivity achieved after 8 h of reaction, following conditions selected from the literature [32].

Although an excess of hydrogen peroxide has been used (ca. 2:1 in relation to nerol), only a poor conversion (ca. 5 %) was obtained in the absence of a catalyst (omitted by simplification). Conversely, in the niobium oxide-catalyzed reactions the nerol was selectively converted to oxidation products (Scheme 2).

The Nb<sub>2</sub>O<sub>5</sub> - 2 h catalyst was much more efficient than other synthesized oxides. The highest conversion (ca. 82 %) and selectivity toward nerol epoxide (ca. 94 %) was achieved after 8 h of reaction. Notably, these results were superior that achieved by niobium oxides prepared by the peroxidation method [52]. Even though nerol epoxide has been the major product in all the reactions, the selectivity toward carbonyl products (i.e., 1b and 2a) was gradually improved when niobium catalysts were synthesized at longer times. Conversely, the terminal double bond of the nerol remained untouched along with the reaction, probably due to the steric hindrance triggered by two methyl groups.

A comparison of the characterization data of niobium oxides and their catalytic activity leads to a conclusion that the surface properties and acidity of niobium oxides played an essential role in this reaction. The most acidic catalyst (Nb<sub>2</sub>O<sub>5</sub> - 2 h; Fig. 5) with the lowest surface area (Table 1) was the most efficient, achieving the highest conversion.

On the other hand, catalysts synthesized at longer periods showed a different selectivity; while the selectivity of aldehydes increased, the selectivity of epoxide products was reduced, which may be assigned to a modification on the catalyst surface.

Balker et al reported that the alcohols are preferentially oxidized by hydrogen peroxide to carbonyl products when Ti silicate (i.e., TS-1) is the catalyst [26]. However, Tatsumi et al. described that this reaction is suppressed if allylic hydroxyl groups are present and, consequently, epoxide becomes the major product [53]. Investigating the geraniol epoxidation with H<sub>2</sub>O<sub>2</sub> over TS-1 catalysts, those authors demonstrated that the epoxidation of allylic alcohols is a hydroxy-assisted reaction. Therefore, based on the literature and experimental data obtained we propose that on niobium-catalyzed oxidation of nerol involves an intermediate as depicted in Scheme 3.

The literature describes the oxidation of geraniol by hydrogen peroxide in tungsten, titanium, or vanadium-catalyzed reactions; on these processes, steps such as the coordination of metal oxide catalyst to the olefin double bond, as well as the peroxidation of the metal are always involved [54]. In general, after the peroxidation step, a three-centered ring intermediate involving the metal oxide and an oxygen atom of peroxide is formed; however, it was omitted in Scheme 3 aiming to do cleaner the reaction. Only the peroxide group (i.e., OOH) bonded to the metal center was depicted herein.

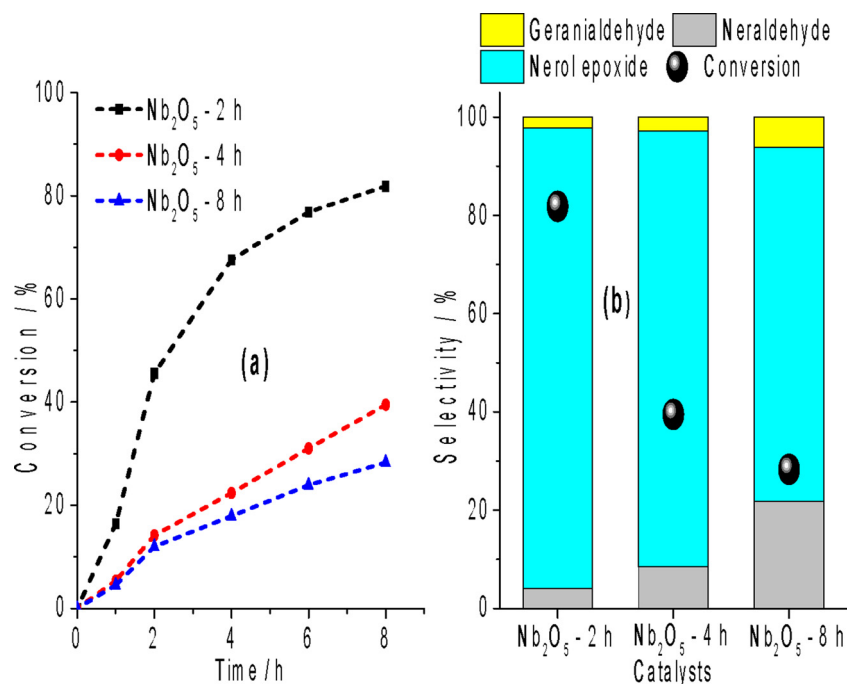
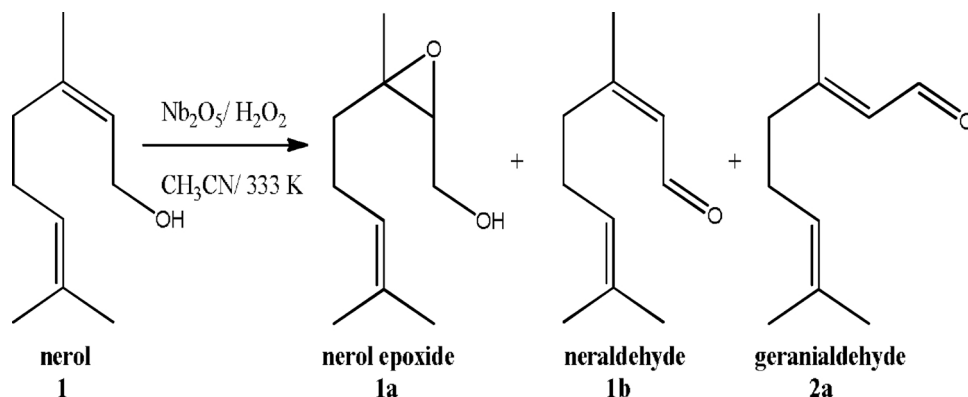


**Fig. 7.** Effect of  $\text{Nb}_2\text{O}_5$  catalyst treatment time on the kinetic curves (a), conversion and products selectivity (b) of nerol oxidation with  $\text{H}_2\text{O}_2$ .<sup>a</sup> Reaction conditions: nerol (1.375 mmol),  $\text{H}_2\text{O}_2$  (2.750 mmol), temperature (333 K), catalyst (4 mol %),  $\text{CH}_3\text{CN}$  (10 mL)

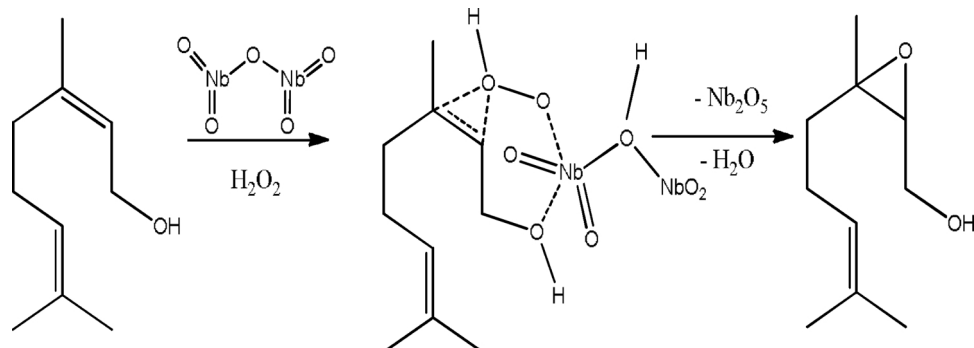


**Scheme 2.** Oxidation products of nerol obtained in  $\text{Nb}_2\text{O}_5$ -catalyzed reactions.

The change in chemoselectivity can be attributed to the coordination of the nerol on the surface of  $\text{Nb}_2\text{O}_5$ . It is very important to highlight that analogously to the described by Adams et al and Kumar et al., we are supposing that the transition state of the epoxidation of nerol involves the coordination of the allylic hydroxyl group to the Nb active site; it means that the double bond interacts with one peroxidic

oxygen atom, not the niobium oxide-oxygen atom [23,55].

The peroxidation step of the niobium catalyst and the interaction with the organic substrate is attributed to the different species of active sites present in the niobium catalyst. Lewis acidic sites and Brønsted acidic sites allow the simultaneous adsorption of the oxidant and the organic substrate even in the presence of water [56].



**Scheme 3.**  $\text{Nb}_2\text{O}_5$ -catalyzed hydroxy-assisted epoxidation of nerol with  $\text{H}_2\text{O}_2$  adapted from [26].

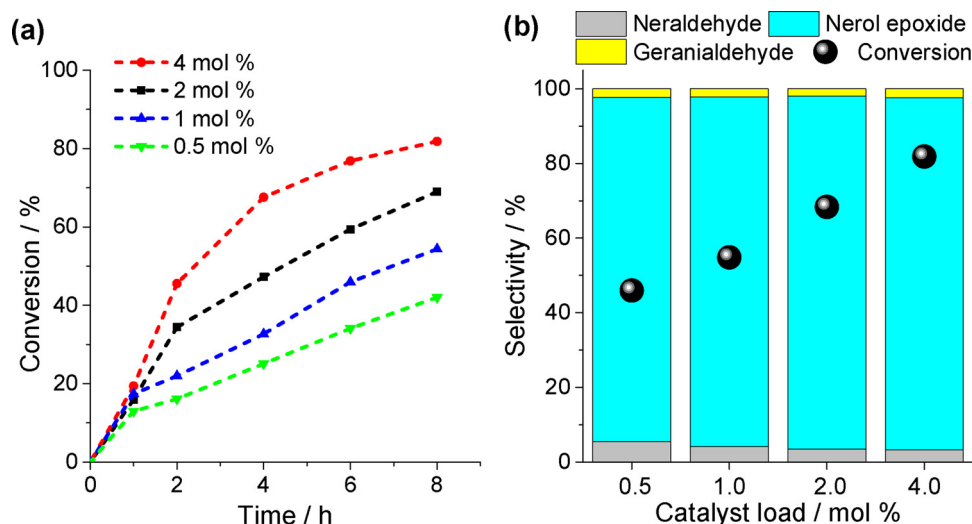


**Fig. 8.** Effect of catalyst load on the kinetic curves (a), conversion and products selectivity (b) of the nerol oxidation with  $\text{H}_2\text{O}_2$  over  $\text{Nb}_2\text{O}_5 - 2 \text{ h}^{\text{a}}$ .  
<sup>a</sup>Reaction conditions: nerol (1.375 mmol),  $\text{H}_2\text{O}_2$  (2.750 mmol), temperature (333 K),  $\text{CH}_3\text{CN}$  (10 mL)

We can conclude that once the  $\text{Nb}_2\text{O}_5 - 2 \text{ h}$  presented a higher Brønsted acidity (see IR spectra and acidity measurements, Figs. 2 and 5), the interaction of nerol hydroxyl group with the peroxidized catalyst is more favorable, therefore, epoxide was the major product (Fig. 7). Conversely, when the catalysts have lower Brønsted acid sites number (i.e., because they were synthesized in 4 or 8 h), the epoxide selectivity is lowered, favoring the formation of the neraldehyde ( $\text{Nb}_2\text{O}_5 - 4$  and 8 h, Fig. 7).

XRD also demonstrated that the  $\text{Nb}_2\text{O}_5 - 2 \text{ h}$  catalyst presented the lowest crystallinity among the three materials. These characteristics positively contributed to improving the interaction of the  $\text{H}_2\text{O}_2$  and nerol with the catalyst surface [17,57]. The  $\text{Nb}_2\text{O}_5 - 2 \text{ h}$  catalyst was selected to study the effect of main reaction parameters due to its better performance.

#### Effects of catalyst load

The impacts of catalyst load were evaluated keeping constant the other variables in the reaction. Fig. 8 shows the kinetic curves, conversion, and selectivity achieved in reactions with a load of catalyst ranging from 2 to 8 mol %.

Although not shown in Fig. 8, a control experiment was carried out without the presence of the catalyst. When nerol and hydrogen peroxide were heated and stirred during 8 h of reaction, no oxidation product or epoxide was detected. It is a guarantee that the formation of these compounds depends on the presence of the  $\text{Nb}_2\text{O}_5 - 2 \text{ h}$  catalyst.

Conversely, while the reactions were performed in the presence of the niobium oxide catalyst, nerol epoxide and the carbonylic products were obtained, with the highest selectivity toward epoxide.

With 4 mol % of catalyst load, the reaction achieved 82 % of conversion. When we performed reactions with higher loads of catalyst, no significant difference was observed in the conversions, which varied from 82 to 87 %. This enhancement of conversion is a consequence of a higher acidic sites number, feasible when a higher concentration is used. Therefore, lower catalysts loading were used (ca. 2.0 – 0.5 mol %). At this range of catalyst load, the reaction conversions were gradually diminished. Notwithstanding, the reaction selectivity remained basically unaltered; nerol epoxide was always the main product (ca. 94 %), and aldehydes of nerol and geraniol were the secondary products. It is evidence that selectivity depends on the nature of the catalyst.

#### Effects of oxidant: substrate ratio

The results for  $\text{Nb}_2\text{O}_5 - 2 \text{ h}$  catalyst in reaction with different amounts of oxidant are presented in Fig. 9. An improvement in the

conversion was obtained using a higher oxidant load. However, this effect was only noticed when the reactions were performed with 4 mol % of catalyst.

The presence of a higher load of oxidant also resulted in an increase in the amount of water in the solution. This aspect changed the chemoselectivity of the reaction, although nerol epoxide has continued to be the main product. The water benefited the isomerization of nerol to geraniol, which was also formed when the proportion of  $\text{H}_2\text{O}_2$ : nerol was 1:2 and 1:3. There was an increase in the selectivity for geranialdehyde. However, the nerol epoxide selectivity was close to 90 %. No significant amount of geraniol epoxide was detected along with the reactions.

#### Effects of reaction temperature

The impacts of temperature on the kinetic curves, conversion, and selectivity of nerol oxidation were assessed using the optimized conditions (ca. 2:1 oxidant: substrate ratio, 4 mol % of catalyst) (Fig. 10).

When the reactions were carried out at different temperatures, an induction period at the process beginning was noticed, mainly at the lowest temperatures. We suppose that at low temperatures, the catalyst peroxidation step is less favored. Consequently, a minimum amount of substrate is consumed within the initial period of reaction. This effect was being suppressed when higher temperatures were used. On the other hand, the reaction selectivity remained almost the same; at the end of the reactions, nerol epoxide was obtained always with a selectivity close to 94 %.

#### Effects of terpenic alcohol structure

The catalytic activity of  $\text{Nb}_2\text{O}_5 - 2 \text{ h}$  was also tested on the oxidation of different terpene alcohols. Fig. 11 displays all the terpenic alcohols investigated; allylic acyclic primary alcohols (nerol and geraniol), allylic acyclic tertiary alcohol (linalool) or cyclic ( $\alpha$ -terpineol) were selected. It is important to note that although the hydroxyl group of tertiary alcohols is not oxidizable (i.e., linalool and  $\alpha$ -terpineol), these substrates have double bonds which may be epoxidized.

Among the evaluated alcohols, only nerol and their geometric isomer geraniol were selectively oxidized, providing their epoxides as main products. Therefore, only the selectivity of these three alcohols is displayed in Fig. 12. The double bond of  $\alpha$ -terpineol remained untouched and no epoxide was detected. This result is reinforcing that the epoxidation is a hydroxy assisted-reaction.

Although linalool has an allylic hydroxyl group likewise geraniol and nerol, it was not epoxidized. It can be attributed to the hysteric

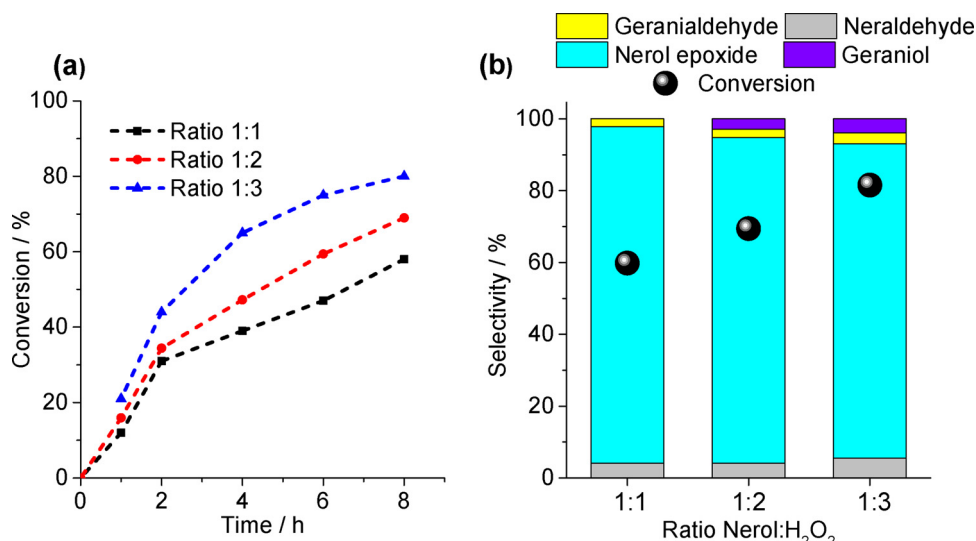


**Fig. 9.** Effect of substrate: oxidant ratio on the kinetic curves (a), conversion and products selectivity (b) of the nerol oxidation by H<sub>2</sub>O<sub>2</sub> in the presence of Nb<sub>2</sub>O<sub>5</sub> - 2 h catalyst<sup>a</sup>.

<sup>a</sup>Reaction conditions: Nerol (1.375 mmol), temperature (333 K), catalyst (2 mol %), CH<sub>3</sub>CN (10 mL)

hindrance provoked by the methyl group, which is bonded to the same carbon atom that the hydroxyl group. On the other hand, these three allylic alcohols have another double bond disubstituted that due to the absence of an allylic hydroxy group and a high steric hindrance remained intact.

The reaction selectivity showed that the oxidation of the hydroxy group of geraniol to aldehyde was easier than nerol. This higher selectivity for aldehyde was a consequence of a lower formation of epoxide; possibly, the formation of the transition state that led to the epoxide more favourably for nerol than geraniol. It is well established that geraniol has a *trans*-ol and nerol a *cis*-ol configuration around the trisubstituted carbon-carbon double bond. Consequently, the interaction of niobium with the hydroxyl group of nerol is more effective.

Although the selectivity obtained herein have been comparable to

those achieved in oxidation reactions carried out over WO<sub>3</sub>-SiO<sub>2</sub> mesoporous catalysts, the conversions were higher even at a lower temperature [25].

#### Recovery and reuse of Nb<sub>2</sub>O<sub>5</sub> - 2 h catalyst

The catalyst was easily recovered from the reaction medium by centrifugation. High recovery rates were achieved (ca. 95 %). Although the conversion did not reach 40 %, the reaction maintained the high selectivity for nerol epoxide (Fig. 13).

To try understanding the reason for the drop in the activity of Nb<sub>2</sub>O<sub>5</sub>-2 h catalyst after it has been reused, we carried out analyses of FT-IR spectroscopy and XRD patterns and compared them with the data obtained from the fresh catalyst.

The IR spectra (Fig. 14) showed a decrease in the intensity of the

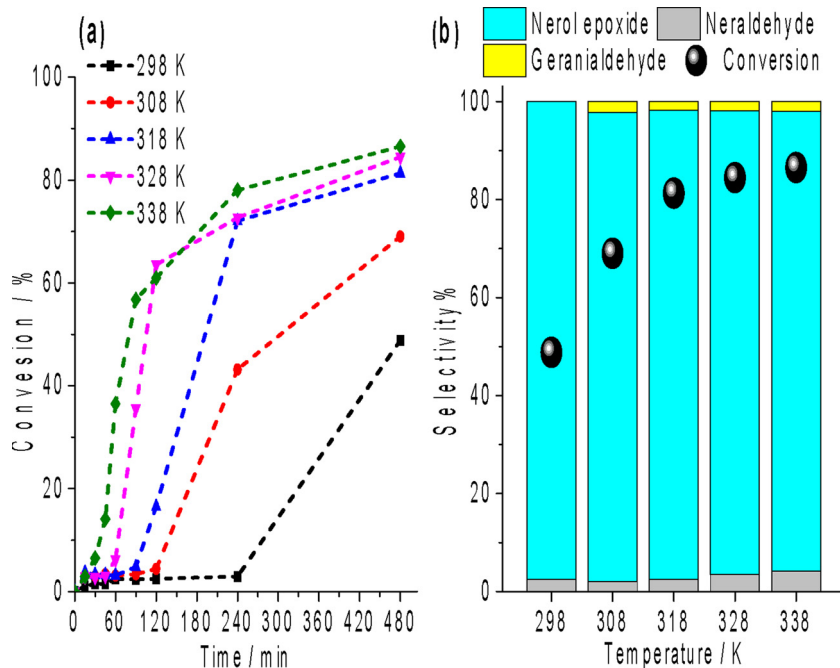


**Fig. 10.** Effects of temperature on the kinetic curves (a), conversion and products selectivity (b) of the nerol oxidation with H<sub>2</sub>O<sub>2</sub> over Nb<sub>2</sub>O<sub>5</sub> - 2 h catalyst.<sup>a</sup>

<sup>a</sup>Reaction conditions: nerol (1.375 mmol), H<sub>2</sub>O<sub>2</sub> (2.750 mmol), catalyst (4 mol %), CH<sub>3</sub>CN (10 mL)

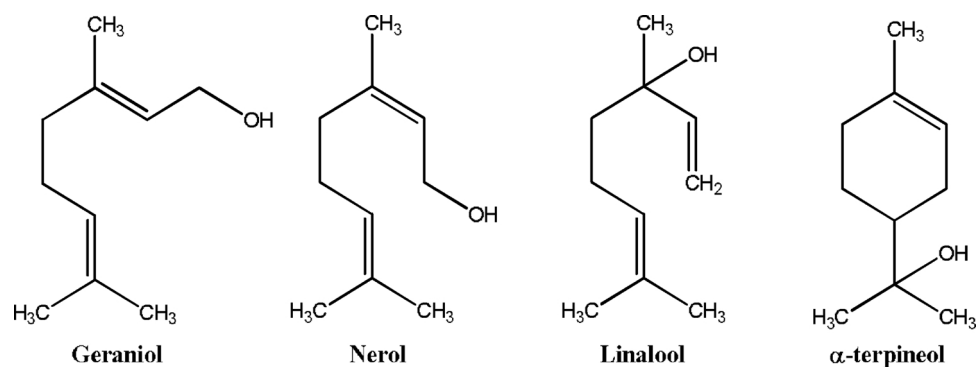


Fig. 11. Structure of terpenic alcohols.

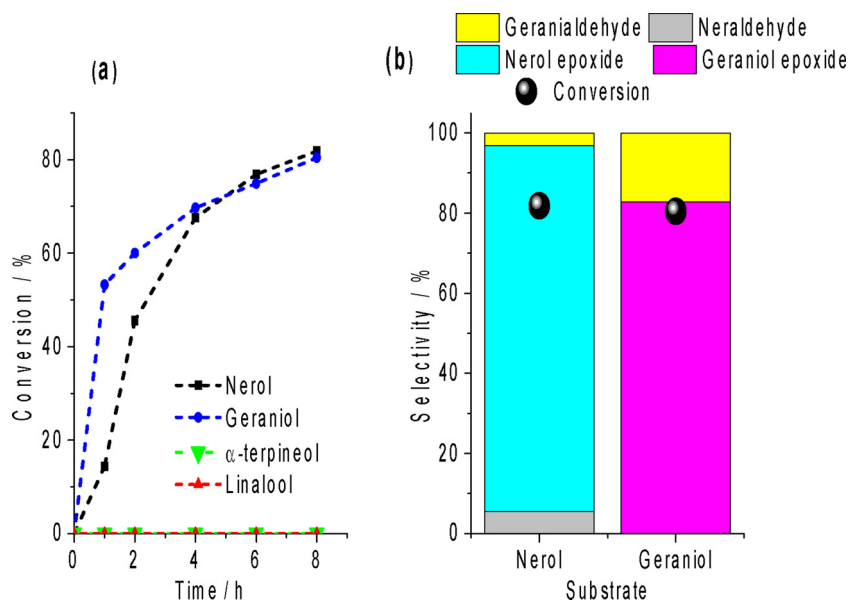


Fig. 12. Kinetic curves (a), conversion and products selectivity (b) of  $\text{Nb}_2\text{O}_5$  - 2 h-catalyzed terpenic alcohols oxidation by  $\text{H}_2\text{O}_2$ <sup>a</sup>.  
<sup>a</sup>Reaction conditions: terpenic alcohol (1.375 mmol),  $\text{H}_2\text{O}_2$  (2.750 mmol), temperature (333 K), catalyst (4 mol %),  $\text{CH}_3\text{CN}$  (10 mL)

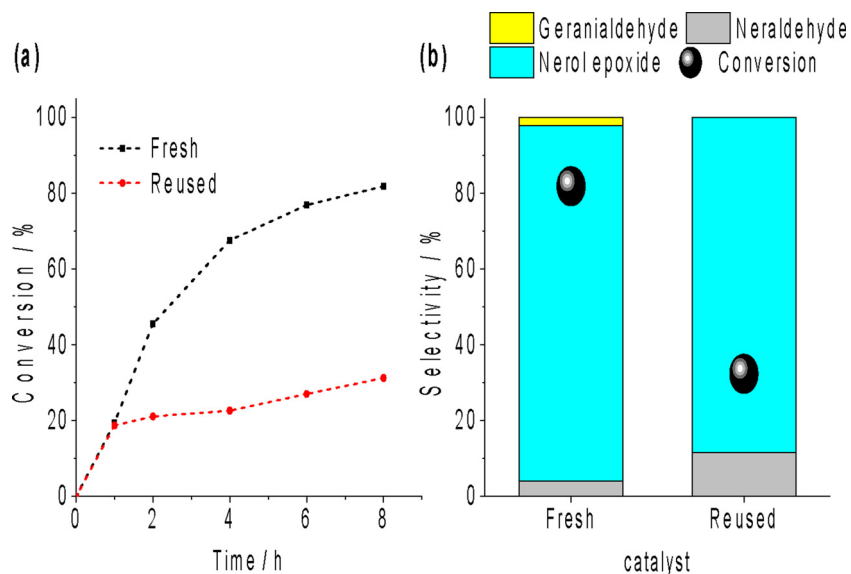


Fig. 13. Conversion (a) and selectivity (b) of nerol oxidation reactions with  $\text{H}_2\text{O}_2$  in the presence of  $\text{Nb}_2\text{O}_5$  - 2 h (fresh and reused). The black bar on b graphic represents the conversion at 8 h of reaction<sup>a</sup>.  
<sup>a</sup>Reaction conditions: Nerol (1.375 mmol),  $\text{H}_2\text{O}_2$  (2.750 mmol), temperature (333 K), catalyst (4 mol %),  $\text{CH}_3\text{CN}$  (10 mL)

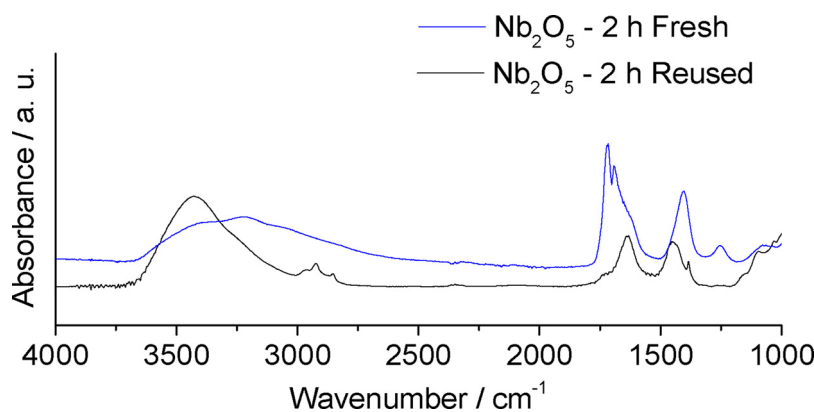


Fig. 14. FT-IR spectra obtained from Nb<sub>2</sub>O<sub>5</sub> - 2 h fresh and reused catalysts.

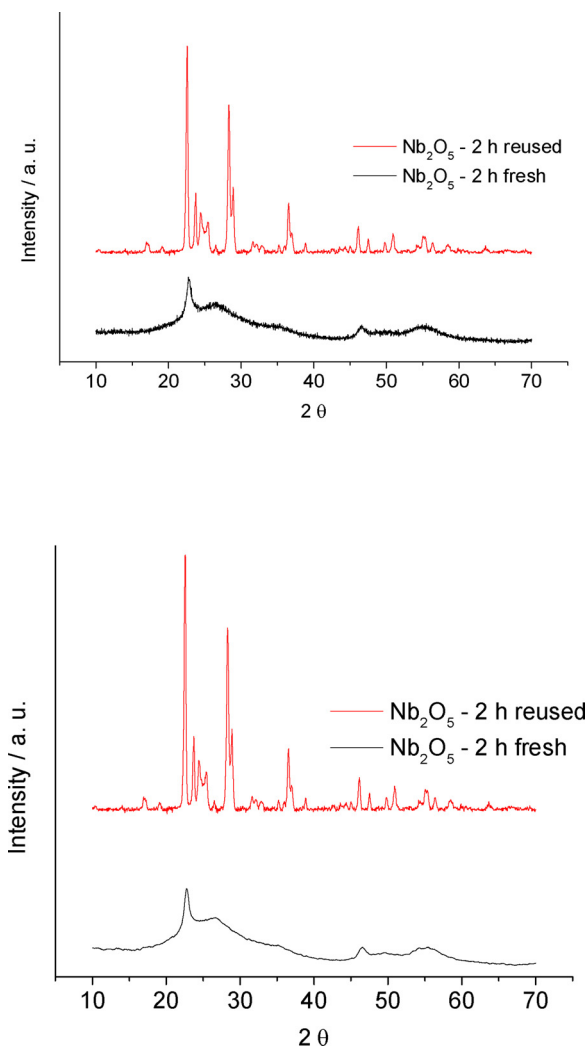


Fig. 15. XRD patterns obtained from the Nb<sub>2</sub>O<sub>5</sub> - 2 h fresh and reused catalysts.

band regarding the binding of Nb to the OH<sup>-</sup> groups, at wavenumbers 1700 cm<sup>-1</sup>, after the catalyst has been reused. On the basis of the literature, it is correct to state that it is suggestive that there are less OH<sup>-</sup> groups on the catalyst surface [41]

On the other hand, the analysis of the XRD patterns revealed an increase in crystallinity for the reused catalyst (Fig. 15). According to Ziolk et al, an increase of this parameter is directly related to the loss of availability of OH<sup>-</sup> groups on the catalyst surface [17]. The catalytic activity of the niobium oxides varies according to the number of

hydroxyl groups present on the catalyst surface; with less hydroxyl groups, the catalyst has lower activity [17,41].

Therefore, we can conclude that the main change that occurred on the Nb<sub>2</sub>O<sub>5</sub>-2 h catalyst after it has been recovered and reused was the lower availability of hydroxyl groups on their surface. The loss of surface hydroxyl groups suggests that the catalyst also had their strength acidity reduced. Moreover, the interaction with the hydrogen peroxide oxidant may be also compromised, triggering a significant decrease in the activity of the reused catalyst in subsequent nerol oxidation reactions. Literature has described that the hydroxyl groups may have the ability to bind to H<sub>2</sub>O<sub>2</sub> molecules generating different reactive oxygen species, which may favor the activity of these niobium oxides in oxidation reactions [40,42].

Finally, an additional test was carried to verify the possible leaching of catalyst could be also has contributed to their deactivation. The niobium oxide was stirred and heated in the presence of the oxidant in solution without the presence of the nerol. After the removal of solid catalyst through hot filtration, nerol and oxidant were added to the supernatant and the reaction monitored during 8 h. No conversion was noticed as well as no oxidation product was detected. It is a guarantee that the Nb<sub>2</sub>O<sub>5</sub>-catalyzed reaction was truly heterogeneous. Besides the high recovery rate of catalyst achieved in the reuse, this evidence assures that the catalyst is almost insoluble in the reaction.

## Conclusions

The microwave-assisted hydrothermal method was efficient to produce niobium oxides with controlled morphological properties, which demonstrated to be effective catalysts for the selective epoxidation of allylic terpenic alcohols with hydrogen peroxide. Reactions were conveniently carried out in the presence of a solid catalyst (i.e., Nb<sub>2</sub>O<sub>5</sub> - 2 h), and hydrogen peroxide, an inexpensive and green oxidant.

Notwithstanding its lowest surface area, the most active catalyst was Nb<sub>2</sub>O<sub>5</sub> - 2 h, a consequence of the highest amount of strongest acidic sites, which favored the interaction of the catalyst surface with terpenic alcohol. XRD patterns, IR and Raman spectra obtained from niobium oxides assisted in the interpretation of catalytic test results through the acidity presented by the materials.

Likewise described for tungsten or titanium catalyzed reactions, the epoxidation of allylic terpenic alcohols with H<sub>2</sub>O<sub>2</sub> is a hydroxy-assisted reaction. Therefore, the Nb<sub>2</sub>O<sub>5</sub> - 2 h catalyst that had a higher number of Brønsted acidic site was the most active. The reactivity of other terpenic alcohols was also evaluated. Linalool, another allylic alcohol was unreactive, the consequence of high steric hindrance of the tertiary hydroxy group. The double bond of  $\alpha$ -terpineol was not epoxidized, possibly due to the absence of an allylic hydroxy group. The stereochemistry of nerol makes it more reactive than geraniol, consequently, higher conversion and selectivity toward epoxide was achieved. The reusability of catalysts was investigated. High recovery rates (ca. 95%)

were obtained. After recovery, the solid catalyst was reused without loss of selectivity, however, there was a significant decrease of conversion. Infrared spectroscopy analysis and XRD patterns of the reused catalyst showed that there was a loss of hydroxyl groups on the catalyst surface, which compromised their activity.

### Credit author statement

I, Marcio Jose da Silva, corresponding author of this paper, state that:

The corresponding author is responsible for ensuring that the descriptions are accurate and agreed by all authors.

Authors equally contributed in the paper.

### Declaration of Competing Interest

The authors declare that they have no known competing financial interests or personal relationships that could have appeared to influence the work reported in this paper.

### Acknowledgements

The authors thank the Federal University of Viçosa, the PPGMQ-MG, and the development agencies CNPq and FAPEMIG. This study was financed in part by the Coordenação de Aperfeiçoamento de Pessoal de Nível Superior – Brasil (CAPES) – Finance Code 001.

### References

- [1] F. Cavani, N. Ballarini, S. Luciani, Catalysis for society: towards improved process efficiency in catalytic selective oxidations, *Top. Catal.* 52 (2009) 935–947, <https://doi.org/10.1007/s11244-009-9244-y>.
- [2] W. Schwab, C. Fuchs, F. Huang, Transformation of terpenes into fine chemicals, *Eur. J. Lipid Sci. Technol.* 115 (2013) 3–8, <https://doi.org/10.1002/ejlt.201200157>.
- [3] P. Gallezot, Catalytic routes from renewables to fine chemicals, *Catal. Today* 121 (2007) 76–91, <https://doi.org/10.1016/j.cattod.2006.11.019>.
- [4] M. Besson, P. Gallezot, C. Pinel, Conversion of biomass into chemicals over metal catalysts, *Chem. Rev.* 114 (2013) 1827–1870, <https://doi.org/10.1021/cr4002269>.
- [5] P.T. Anastas, M.M. Kirchhoff, Origins, current status, and future challenges of green chemistry, *Acc. Chem. Res.* 35 (2002) 686–694, <https://doi.org/10.1021/ar010065m>.
- [6] L.A.S. Viana, G.R.N. Da Silva, M.J. Da Silva, A highly selective  $\text{Na}_2\text{WO}_4$ -Catalyzed oxidation of terpenic alcohols by hydrogen peroxide, *Catal. Lett.* 148 (2018) 374–382, <https://doi.org/10.1007/s10562-017-2246-7>.
- [7] K.A.D. Swift, Catalytic transformations of the major terpene feedstocks, *Top. Catal.* 27 (2004) 143–155, <https://doi.org/10.1023/B:TOCA.0000013549.60930.da>.
- [8] E.J. Lenardao, G.V. Botteselle, F. De Azambuja, G. Perin, R.G. Jacob, Citronellal as key compound in organic synthesis, *Tetrahedron* 63 (2007) 6671–6712, <https://doi.org/10.1016/j.tet.2007.03.159>.
- [9] S. Serra, D. De Simeis, Two complementary synthetic approaches to the enantiomeric forms of the chiral building block (2, 6, 6-Trimethyltetrahydro-2H-pyran-2-yl) methanol: application to the stereospecific preparation of the natural flavor linaloyl oxide, *Catalysts* 8 (2018) 362, <https://doi.org/10.3390/catal8090362>.
- [10] J.L.F. Monteiro, C.O. Veloso, Catalytic conversion of terpenes into fine chemicals, *Top. Catal.* 27 (2004) 169–180, <https://doi.org/10.1023/B:TOCA.0000013551.99872.8d>.
- [11] M.J. Da Silva, D.A.M. Ayala, Unravelling transition metal-catalyzed terpenic alcohol esterification: a straightforward process for the synthesis of fragrances, *Catal. Sci. Technol.* 6 (2016) 3197–3207, <https://doi.org/10.1039/C5CY01538C>.
- [12] Z. Guo, B. Liu, Q. Zhang, W. Deng, Y. Wang, Y. Yang, Recent advances in heterogeneous selective oxidation catalysis for sustainable chemistry, *Chem. Soc. Rev.* 43 (2014) 3480–3524, <https://doi.org/10.1039/C3CS60282F>.
- [13] L.A.F. Azevedo, L. Menini, E.V. Gusevskaya, Functionalization of the naturally occurring linalool and nerol by the palladium catalyzed oxidation of their trisubstituted olefinic bonds, *J. Mol. Catal. A Chem.* 426 (2017) 429–434, <https://doi.org/10.1016/j.molcata.2016.07.033>.
- [14] S. Sakaguchi, Y. Nishiyama, Y. Ishii, Selective oxidation of monoterpenes with hydrogen peroxide catalyzed by peroxotungstophosphate (PCWP), *J. Org. Chem.* 61 (1996) 5307–5311, <https://doi.org/10.1021/jo960275q>.
- [15] J. Piera, J. Baekvall, Catalytic oxidation of organic substrates by molecular oxygen and hydrogen peroxide by multistep electron transfer—a biomimetic approach, *Angew. Chem., Int. Ed.* 47 (2008) 3506–3523, <https://doi.org/10.1002/anie.200700604>.
- [16] V.M. Vaschetti, A.L. Cánepa, D. Barrera, K. Sapag, G.A. Eimer, S.G. Casuscelli, Limonene oxyfunctionalization over Cu-modified silicates employing hydrogen peroxide and t-Butyl hydroperoxide: reaction pathway analysis, *Mol. Catal.* 481 (2018) 110234, <https://doi.org/10.1016/j.mcat.2018.11.005>.
- [17] M. Ziolek, I. Sobczak, P. Decyk, K. Sobanska, P. Pietrzyk, Z. Sojka, Search for reactive intermediates in catalytic oxidation with hydrogen peroxide over amorphous niobium(V) and tantalum(V) oxides, *Appl. Catal. B* 164 (2015) 288–296, <https://doi.org/10.1016/j.apcatb.2014.09.024>.
- [18] R. Noyori, M. Aoki, K. Sato, Green oxidation with aqueous hydrogen peroxide, *Chem. Commun.* 16 (2003) 1977–1986, <https://doi.org/10.1039/B303160H>.
- [19] W. Zhao, Y. Zhang, B. Ma, Y. Ding, W. Qiu, Oxidation of alcohols with hydrogen peroxide in water catalyzed by recyclable Keggin-type tungstoborate catalyst, *Catal. Commun.* 11 (2010) 527–531, <https://doi.org/10.1016/j.catcom.2009.12.010>.
- [20] C.B. Vilanculo, M.J. da Silva, S.O. Ferreira, M.G. Teixeira, A rare oxidation of camphene to acid and aldehyde in the presence of Lacunar Keggin heteropoly salts, *Mol. Catal.* 478 (2019) 110589, <https://doi.org/10.1016/j.mcat.2019.110589>.
- [21] D.E. De Vos, B.F. Sels, P.A. Jacobs, Practical heterogeneous catalysts for epoxide production, *Adv. Synth. Catal.* 345 (2003) 457–473, <https://doi.org/10.1002/adsc.200390051>.
- [22] C. Wang, H. Yamamoto, Tungsten-catalyzed asymmetric epoxidation of allylic and homoallylic alcohols with hydrogen peroxide, *J. Am. Chem. Soc.* 136 (2014) 1222–1225, <https://doi.org/10.1021/ja411379e>.
- [23] R. Kumar, G.C.G. Pais, B. Pandey, P. Kumar, Hydroxy-assisted chemo- and stereoselective epoxidation catalysed by a titanium silicate molecular sieve (TS-1)/ $\text{H}_2\text{O}_2$  system, *J. Chem. Soc. Chem. Commun.* 13 (1995) 1315–1316, <https://doi.org/10.1039/C39950001315>.
- [24] N. Marin-Astorga, J.J. Martinez, G. Borda, J. Cubillos, D.N. Suarez, H. Rojas, Control of the chemoselectivity in the oxidation of geraniol over lanthanum, titanium and niobium catalysts supported on mesoporous silica MCM-41, *Top. Catal.* 55 (2012) 620–624, <https://doi.org/10.1007/s11244-012-9840-0>.
- [25] F. Somma, G. Strukul, Oxidation of geraniol and other substituted olefins with hydrogen peroxide using mesoporous, sol-gel-made tungsten oxide-silica mixed oxide catalysts, *J. Catal.* 227 (2004) 344–351, <https://doi.org/10.1016/j.jcat.2004.07.006>.
- [26] M. Dusi, T. Mallat, A. Baiker, Epoxidation of functionalized olefins over solid catalysts, *Catal. Rev.* 42 (2000) 213–278, <https://doi.org/10.1081/CR-100100262>.
- [27] M.J. Da Silva, P.H.S. Andrade, S.O. Ferreira, C.B. Vilanculo, C.M. Oliveira, Monolacunary  $\text{K}_8\text{SiW}_{11}\text{O}_{39}$ -Catalyzed terpenic alcohols oxidation with hydrogen peroxide, *Catal. Lett.* 148 (2018) 2516–2527, <https://doi.org/10.1007/s10562-018-2434-0>.
- [28] E.L. Moreno, K. Rajagopal, Challenges of catalysis acidity in solids, *Quím. Nova* 32 (2009) 538–542, <https://doi.org/10.1590/S0100-40422009000200044>.
- [29] A. Esteves, L.C.A. Oliveira, T.C. Ramalho, M. Goncalves, A.S. Anastácio, H.W.P. Carvalho, New materials based on modified synthetic  $\text{Nb}_2\text{O}_5$  as photocatalyst for oxidation of organic contaminants, *Catal. Commun.* 10 (2008) 330–332, <https://doi.org/10.1016/j.catcom.2008.09.012>.
- [30] A.C. Silva, D.Q.L. Oliveira, L.C.A. Oliveira, A.S. Anastácio, T.C. Ramalho, J.H. Lopes, H.W.P. Carvalho, C.E.R. Torres, Nb-containing hematites  $\text{Fe}_{2-x}\text{Nb}_x\text{O}_3$ : the role of  $\text{Nb}^{5+}$  on the reactivity in presence of the  $\text{H}_2\text{O}_2$  or ultraviolet light, *Appl. Catal. A Gen.* 357 (2009) 79–84, <https://doi.org/10.1016/j.apcata.2009.01.014>.
- [31] C. Tiozzo, C. Bisio, F. Carniato, M. Guidotti, Grafted non-ordered niobium-silica materials: versatile catalysts for the selective epoxidation of various unsaturated fine chemicals, *Catal. Today* 235 (2014) 49–57, <https://doi.org/10.1016/j.cattod.2014.02.027>.
- [32] C. Tiozzo, C. Palumbo, R. Psaro, C. Bisio, F. Carniato, A. Gervasini, P. Carniti, M. Guidotti, The stability of niobium-silica catalysts in repeated liquid-phase, epoxidation tests: a comparative evaluation of in-framework and grafted mixed oxides, *Inorg. Chim. Acta Rev.* 431 (2015) 190–196, <https://doi.org/10.1016/j.ica.2015.01.048>.
- [33] J.V. Coelho, L.C.A. Oliveira, F.C.C. Moura, P.P. De Souza, C.A. Silva, K.B. Batista, M.J. Da Silva,  $\beta$ -pinene oxidation by hydrogen peroxide catalyzed by modified niobium-MCM, *Appl. Catal. A Gen.* 419 (2012) 215–220, <https://doi.org/10.1016/j.apcata.2012.01.032>.
- [34] W.M. Ventura, D.C. Batalha, H.V. Fajardo, J.G. Taylor, N.H. Marins, B.S. NoreMBERG, T. Tańskic, N.L.V. Carreño, Low temperature liquid phase catalytic oxidation of aniline promoted by niobium pentoxide micro and nanoparticles, *Catal. Commun.* 99 (2017) 135–140, <https://doi.org/10.1016/j.catcom.2017.06.004>.
- [35] D.C. Batalha, S.C. Luz, J.G. Taylor, H.V. Fajardo, B.S. NoreMBERG, I.J.S. Cherubin, R.M. Silva, M.R.F. Gonçalves, C.P. Bergmann, A. Valentini, N.L.V. Carreño, Application of  $\text{Al}_2\text{O}_3/\text{AlNbO}_4$  in the oxidation of aniline to azoxybenzene, *Chem. Pap.* 74 (2020) 543–553, <https://doi.org/10.1007/s11696-019-00897-5>.
- [36] J. Wan, P. Yang, G. Xiaolin, R. Zhou, Investigation on the structure-activity relationship of  $\text{Nb}_2\text{O}_5$  promoting  $\text{CeO}_2\text{-CrO}_x\text{-Nb}_2\text{O}_5$  catalysts for 1,2-dichloroethane elimination, *Mol. Catal.* 470 (2019) 75–81, <https://doi.org/10.1016/j.mcat.2019.03.010>.
- [37] N.K. Gupta, A. Fukuoka, K. Nakajima, Amorphous  $\text{Nb}_2\text{O}_5$  as a selective and reusable catalyst for furfural production from xylose in biphasic water and toluene, *ACS Catal.* 7 (2017) 2430–2436, <https://doi.org/10.1021/acscatal.6b03682>.
- [38] N.H. Marins, C.T. Meeres, R.M. Silva, C.P. Ruas, A.S. Takimi, N.L. Carreño, F.A. Oglitari, Radiopaque dental adhesive with addition of niobium pentoxide nanoparticles, *Polym. Bull. Berl. (Berl)* 75 (2018) 2301–2314, <https://doi.org/10.1007/s00289-017-2150-8>.
- [39] W.M. Ventura, D.C. Batalha, H.V. Fajardo, J.G. Taylor, N.H. Marins, B.S. NoreMBERG, T. Tańskic, N.L.V. Carreño, Low temperature liquid phase catalytic oxidation of aniline promoted by niobium pentoxide micro and nanoparticles, *Catal. Commun.* 99 (2017) 135–140, <https://doi.org/10.1016/j.catcom.2017.06.004>.

- [40] M. Thommes, K. Kaneko, A.V. Neimark, J.P. Olivier, F.R. Reinoso, J. Rouquerol, K.S. Sing, Physisorption of gases, with special reference to the evaluation of surface area and pore size distribution (IUPAC Technical Report), *Pure Appl. Chem.* 87 (2015) 1051–1069, <https://doi.org/10.1515/pac-2014-1117>.
- [41] T. Athar, A. Hashmi, A. Al-Hajry, Z.A. Ansari, S.G. Ansari, One-pot synthesis and characterization of Nb<sub>2</sub>O<sub>5</sub> nanopowder, *J. Nanosci. Nanotechnol.* 12 (2012) 7922–7926, <https://doi.org/10.1166/jnn.2012.6645>.
- [42] D.C. Castro, R.P. Cavalcante, J. Jorge, M.A. Martinez, L. Oliveira, G.A. Casagrande, A. Machulek Jr, Synthesis and characterization of mesoporous Nb<sub>2</sub>O<sub>5</sub> and its application for photocatalytic degradation of the herbicide methylviologen, *J. Braz. Chem. Soc.* 27 (2016) 303–313, <https://doi.org/10.5935/0103-5053.20150244>.
- [43] M. Ziolk, I. Sobczak, P. Decyk, L. Wolski, The ability of Nb<sub>2</sub>O<sub>5</sub> and Ta<sub>2</sub>O<sub>5</sub> to generate active oxygen in contact with hydrogen peroxide, *Catal. Commun.* 37 (2013) 85–91, <https://doi.org/10.1016/j.catcom.2013.03.032>.
- [44] R. Brayner, F. Bozon-Verduraz, Niobium pentoxide prepared by soft chemical routes: morphology, structure, defects and quantum size effect, *Phys. Chem. Chem. Phys.* 5 (2003) 1457–1466, <https://doi.org/10.1039/B210055J>.
- [45] R. Turco, A. Aronnc, P. Carniti, A. Gervasini, L. Minieric, P. Pernicec, R. Tessera, R. Vitiello, M. Di Serio, Influence of preparation methods and structure of niobium oxide-based catalysts in the epoxidation reaction, *Catal. Today* 254 (2015) 99–103, <https://doi.org/10.1016/j.cattod.2014.11.033>.
- [46] I. Nowak, M. Ziolk, Niobium compounds: preparation, characterization, and application in heterogeneous catalysis, *Chem. Rev.* 99 (1999) 3603–3624, <https://doi.org/10.1021/cr9800208>.
- [47] O.F. Lopes, E.C. Paris, C. Ribeiro, Synthesis of Nb<sub>2</sub>O<sub>5</sub> nanoparticles through the oxidant peroxide method applied to organic pollutant photodegradation: a mechanistic study, *Appl. Catal. B* 144 (2014) 800–808, <https://doi.org/10.1016/j.apcatb.2013.08.031>.
- [48] S.M. Maurer, E.I. Ko, Structural and acidic characterization of niobia aerogels, *J. Catal.* 135 (1992) 125–134, [https://doi.org/10.1016/0021-9517\(92\)90274-L](https://doi.org/10.1016/0021-9517(92)90274-L).
- [49] S.K.N. Ayudhya, A. Soottitantawat, P. Praserttham, C. Satayaprasert, Effect of aging on the properties of mesoporous niobium oxide, *Mater. Chem. Phys.* 110 (2008) 387–392, <https://doi.org/10.1016/j.matchemphys.2008.02.027>.
- [50] L.R. Pizzio, M.N. Blanco, A contribution to the physicochemical characterization of nonstoichiometric salts of tungstosilicic acid, *Microporous Mesoporous Mater.* 103 (2007) 40–47, <https://doi.org/10.1016/j.micromeso.2007.01.036>.
- [51] N.H. Marins, B.E.J. Lee, R.M. Silva, A. Raghavan, N.L.V. Carreno, K. Grandfield, Niobium pentoxide and hydroxyapatite particle loaded electrospun polycaprolactone/gelatin membranes for bone tissue engineering, *Colloids Surf. B Biointerfaces* 182 (2019) 110386, <https://doi.org/10.1016/j.colsurfb.2019.110386>.
- [52] J. Cubillos, J. Martínez, H. Rojas, N. Marín-Astorga, Oxidation of geraniol using niobia modified with hydrogen peroxide, *Rev. Fac. Ing., Univ. Antioquia* 91 (2019) 106–112, <https://doi.org/10.17533/udea.redin.n91a10>.
- [53] T. Tatsumi, M. Yako, M. Nakamura, Y. Yuhara, H. Tominaga, Effect of alkene structure on selectivity in the oxidation of unsaturated alcohols with titanium silicalite-1 catalyst, *J. Mol. Catal. A Chem.* 78 (1993) L41–L45.
- [54] M. Aminia, M.M. Haghdoostb, M. Bagherzadeh, Monomeric and dimeric oxido-peroxido tungsten(VI) complexes in catalytic and stoichiometric epoxidation, *Coord. Chem. Rev.* 268 (2014) 83–100, <https://doi.org/10.1016/j.ccr.2014.01.035>.
- [55] W. Adam, A. Corma, T.I. Reddy, M. Renz, Diastereoselective catalytic epoxidation of chiral allylic alcohols by the TS-1 and Ti-β zeolites: evidence for a hydrogen-bonded, peroxy-type loaded complex as oxidizing species, *J. Org. Chem.* 62 (1997) 3631–3637, <https://doi.org/10.1021/jo970364i>.
- [56] I.W.C.E. Arends, R.A. Sheldon, Activities and stabilities of heterogeneous catalysts in selective liquid phase oxidations: recent developments, *Appl. Catal. A Gen.* 212 (2001) 175–187, [https://doi.org/10.1016/S0926-860X\(00\)00855-3](https://doi.org/10.1016/S0926-860X(00)00855-3).
- [57] L.C.A. Oliveira, N.T. Costa, J.R. Pliego Jr, A.C. Silva, P.P. Souza, P.S.O. Patrício, Amphiphilic niobium oxyhydroxide as a hybrid catalyst for sulfur removal from fuel in a biphasic system, *Appl. Catal. B* 147 (2014) 43–48, <https://doi.org/10.1016/j.apcatb.2013.08.003>.